

Modeling the effect of Phosphorus dose loss at the SiO₂ interface on CMOS device characteristics

H.-H. Vuong^a, C. S. Rafferty^a, J. R. McMacken^b, J. Ning^b, and S. Chaudhry^b

(a) Bell Laboratories, Lucent Technologies, Murray Hill, New Jersey 07974, USA

(b) Bell Laboratories, Lucent Technologies, Orlando, Florida 32819, USA

Abstract--A model for the phosphorus dose loss effect is developed and incorporated into the process simulator PROPHET. The dose loss model is applied consistently with the Transient Enhanced Diffusion and the segregation models in PROPHET to provide doping profiles used by device simulator PADRE in simulations of NMOS, PMOS, and isolation structures for actual VLSI technologies. Comparison of the simulated and measured device characteristics and their dependence on substrate bias and structure geometry shows good agreement, and furthermore highlights the importance of the dose loss phenomenon in these structures.

I. INTRODUCTION

Recent experimental works have shown that the SiO₂ to Si interface can act as a sink for phosphorus [1-4]. In particular, Griffin et al. [1] showed that the phosphorus dose loss could be magnified by the Transient Enhanced Diffusion (TED) effect to be as much as 50% of the initial implant dose. In this study, we have developed and incorporated a new model for the phosphorus dose loss at the SiO₂ interface into the process simulator PROPHET [5,6]. Simulations of various CMOS devices and isolation structures were performed subsequently using device simulator PADRE [5] in conjunction with PROPHET, and the results compared with experimental data to gauge the effect of the phosphorus dose loss phenomenon on these devices.

II. PHOSPHORUS DOSE LOSS MODEL

To model the phosphorus dose loss at the SiO₂ interface, it is assumed that there is a maximum of Q_{sites} trap sites at the interface. During both inert and oxidizing anneals, some of the phosphorus dopants in silicon become trapped at these sites and become electrically inactive. These trapped dopants are assumed to make up an interfacial dose rather than contributing to the dopant concentration in the bulk oxide. The flux of the dopants arriving from bulk silicon to the trap sites, denoted as F_{trap} , is assumed to be described by (1):

$$F_{\text{trap}} = r_p C_P^I (1 - Q_{\text{trapped}} / Q_{\text{sites}}) \quad (1)$$

where r_p in cm s^{-1} is the phosphorus loss rate, C_P^I in cm^{-3} is the active phosphorus concentration in silicon at the interface, Q_{trapped} is the areal concentration of the trapped interfacial dose in cm^{-2} . F_{trap} is thus zero when all the trap sites are filled. The form of F_{trap} for phosphorus is similar to that of arsenic and BF₂ which had been incorporated previously into PROPHET [7]. Q_{sites} is set at $3 \times 10^{14} \text{ cm}^{-2}$, which is the maximum dose loss observed in [1]. The value of r_p was obtained from optimizing the agreement for our device results,

$$r_p = 1.43 \times 10^2 \times \exp(-1.75 / kT) \text{ cm s}^{-1} \quad (2)$$

Equation (1) was added to the set of Partial Differential Equations (PDEs) in PROPHET which solved for the dopant distribution at each time step. The PDEs also include the segregation flux responsible for the phosphorus pile-up at the SiO₂ interface during oxidation (with segregation coefficient of 10), as well as equations describing the coupled fluxes of the point defects and dopants to simulate TED (the "+1" model [8] was used for the initial net excess interstitial distribution). The TED effect, in addition to enhancing overall diffusion, causes pile-up of the affected dopants even during inert anneal [6]. Thus, for phosphorus both segregation and TED effects contribute to pile-up and so enhance the dose loss effect, unlike the situation for boron in which segregation decreases the interfacial concentration in silicon, and unlike arsenic which exhibits small TED effect. Therefore it is crucial that all three effects are simulated consistently and simultaneously for phosphorus.

III. DEVICE RESULTS

A. NMOS DEVICES

A variety of structures in actual CMOS technologies were simulated for which the phosphorus doping was important. The most striking effect of the phosphorus dose loss was observed for a counter-doped NMOS device with a shallow phosphorus implant. Fig. 1 shows the drastic reduction in the simulated phosphorus concentration in silicon when the phosphorus dose loss model is applied. The difference in the simulated profiles with and without the dose loss is caused mainly at the gate oxidation step which immediately follows the shallow phosphorus implant. At the

850°C gate oxidation, TED, Oxidation Enhanced Diffusion (OED), segregation, and the new dose loss effects all play significant parts. Fig. 2 shows the comparison of the simulated NMOS threshold voltage (V_{th}) versus the measured data from actual devices: both the magnitude of V_{th} and its dependence on the substrate bias V_{bs} (the body effect) are in good agreement. In contrast, simulations performed without the dose loss model underestimated V_{th} considerably, by 0.31V at zero V_{bs} and 0.51V at -5V V_{bs} .

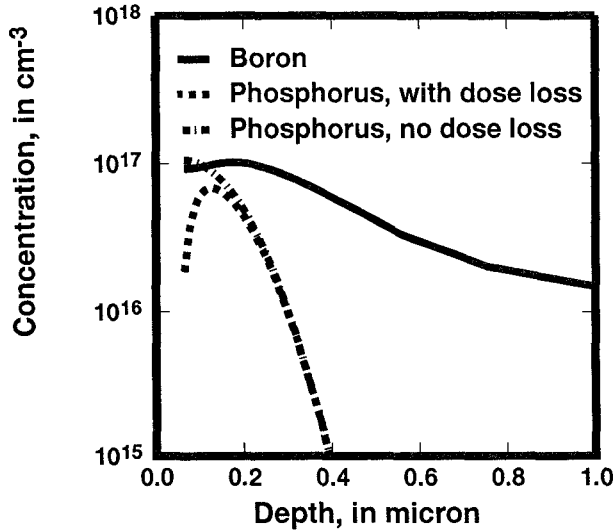


Figure 1: Simulated channel profile of a counter-doped NMOS device. The solid curve is the boron tub-implant. The dash and stipple curves are the phosphorus threshold adjust doping, simulated with and without the new interface dose loss model. The two P curves show a large difference for this process.

B. PMOS DEVICES

Our second set of simulations were for buried-channel PMOS devices in which phosphorus and arsenic implants form the tub doping. The tub implants underwent several anneal sequences which exhibit a large TED effect, including the gate oxidation, LDD anneal, and Source/Drain anneal. A measure of the importance of TED effect in these devices is that simulations without TED showed 400 mV difference in V_{th} compared with simulations with TED. In addition, these buried-channel PMOS devices are very sensitive to small changes in individual dopant profiles because the net dopant profile results from highly compensated n- and p-type dopants (see Fig. 3).

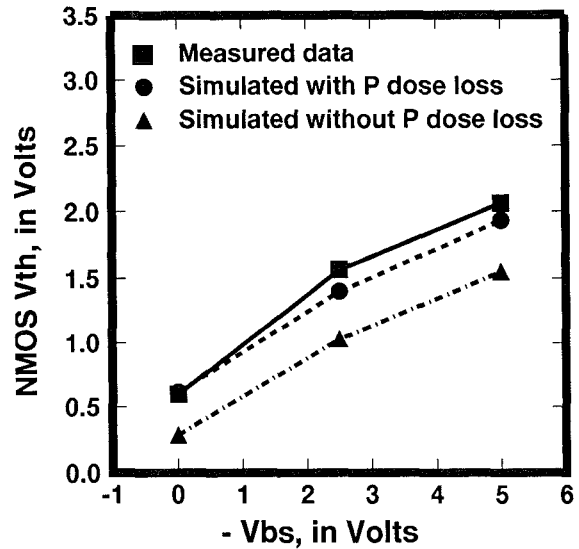


Figure 2: Threshold Voltage V_{th} as a function of the substrate bias V_{bs} for the NMOS device in Figure 1. The measured data (squares) and the data simulated with phosphorus dose loss (circles) agree well. In contrast simulations without the dose loss model (triangles) underestimate V_{th} by 0.31V or more.

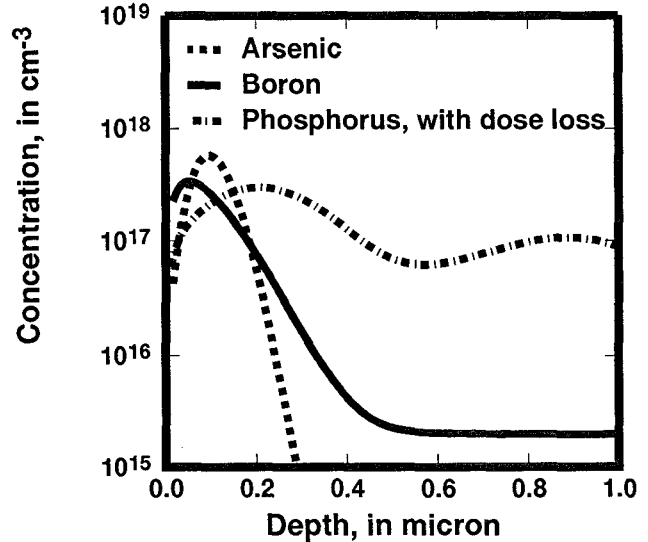


Figure 3: Channel profile of the buried-channel PMOS. The net profile is highly sensitive to changes in each dopant profile. In addition, TED effect is very important in this device, increasing the magnitude of V_{th} by 0.40V.

Fig. 4 compares the simulated to the measured V_{th} values for a long-channel $1.5 \mu m$ and a short-channel $0.35 \mu m$ PMOS device. For the simulated data, PROPHET, employed with phosphorus dose loss (circles in Fig. 4) and without dose loss (triangles), generated the 2D structure and dopant concentrations which are used in the device simulator PADRE to obtain V_{th} and other device characteristics. Both the magnitude and gate-length dependence of V_{th} were better simulated when the phosphorus dose loss was included. In particular, the Short Channel Effect (SCE), defined here as the difference in V_{th} ($1.5 \mu m$) and V_{th} ($0.35 \mu m$), is measured to be 160 mV, and simulated to be 146 mV with the phosphorus dose loss included, and 129 mV without the phosphorus dose loss. Additional simulations without phosphorus dose loss and without TED effect gave almost no SCE (5 mV), showing that (a) TED acts to enhance SCE as previously reported in [7], and (b) both the phosphorus dose loss and TED models must be included in simulations to obtain accurate buried-channel PMOS V_{th} and SCE.

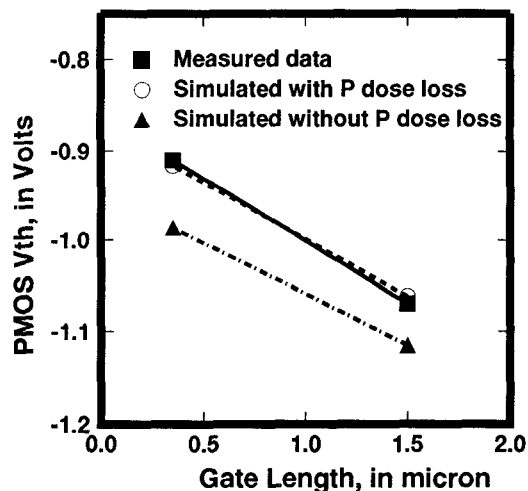


Figure 4: V_{th} of the PMOS depicted in Figure 3, at $1.5 \mu m$ and $0.35 \mu m$ gate lengths (lines are guides for the eye only). Simulations with the dose loss model (circles) match measured data (squares) well in both magnitude and trend (i.e. SCE effect). Simulations without the dose loss (triangles) show significant error in V_{th} magnitude, and a weaker trend in the SCE.

C. ISOLATION STRUCTURES

The third set of simulations concerned a group

of P^+NP^+ isolation structures with varying lithographic isolation gap. In these structures, High Energy phosphorus implants through field oxide form the N-tub doping and BF_2 implant forms the P^+ doping for the source and drain areas. A typical isolation structure and its doping contour lines are shown in Fig. 5(a).

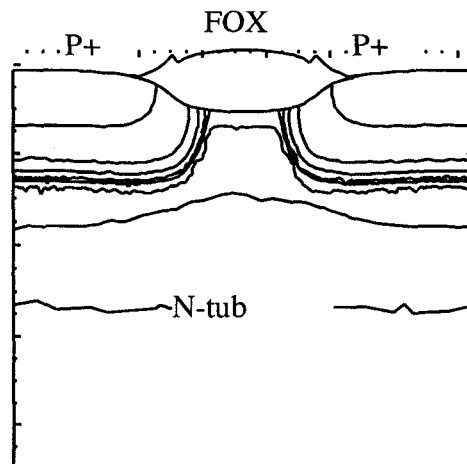


Figure 5a: Isolation structure with doping contours. The field oxide region is shown centre top. Heavily-doped regions on each side of the field oxide are p^+ , and are separated by the phosphorus-doped tub region.

Fig. 5(b) compares the phosphorus doping with and without the dose loss model for the cross-section through the center of the field oxide region, showing a significant difference in the top $0.1 \mu m$.

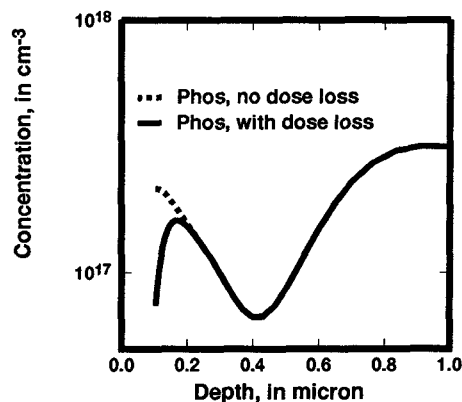


Figure 5b: phosphorus doping profile at the center of the field oxide region, simulated with (solid curve) and without (dotted curve) the dose loss model

PADRE was used to generate device characteristics, the most important being the magnitude of the leakage current between the P⁺ regions, which is determined mainly by the distance between the N-P⁺ lateral junctions. Fig. 6 gives plots of the leakage current I_{ds} as a function of the voltage V_{ds} applied across the P⁺ regions, for isolation gap of 0.4 μm, and phosphorus implant dose of 3x10¹² cm⁻². The difference in the doping profiles shown in Fig. 5(b) resulted in a 27% difference in I_{ds} at V_{ds} = 5V for this structure.

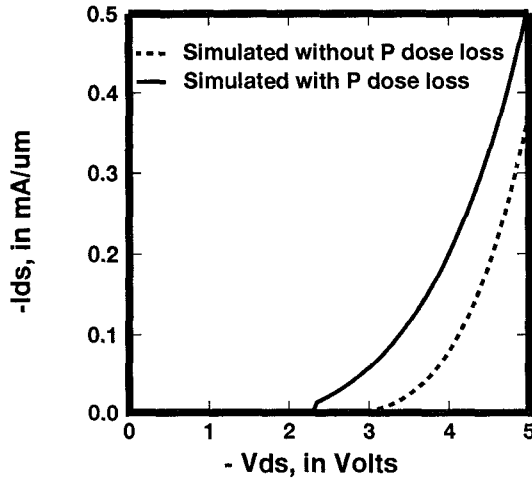


Figure 6: Leakage current I_{ds} vs V_{ds} for isolation structure with a 0.40 μm gap and 3E12 cm⁻² phosphorus implant dose, simulated with (solid curve) and without (dash curve) the dose loss model.

Using the phosphorus dose loss model, a series of isolation structures were simulated with the isolation gap varying from 0.35 μm to 0.70 μm, for phosphorus implant dose of 1x10¹² cm⁻² and 3x10¹² cm⁻². Fig. 7 compares the leakage current at 5V V_{ds} from these simulations with the measured values. Given the measurement lower limit for I_{ds} of 1x10⁻¹¹ A/μm, the agreement is good. In particular, the critical values of the isolation gap, below which the leakage current rises exponentially with decreasing gap, is simulated (measured) to be 0.55 (0.60) μm for phosphorus implant dose of 1x10¹² cm⁻² and 0.50 (0.45) μm for 3x10¹² cm⁻². The agreement is within 0.05 μm, which is the interval between measurements. Simulations without the dose loss model gave worse agreement with measured data (lower I_{ds}) for all points, although the critical gap values were not changed.

IV. CONCLUSION

A new model for phosphorus dose loss at the SiO₂ interface is developed and incorporated into the process simulator PROPHET. The model is then used consistently with TED and segregation effects to simulate the processing

and device characteristics of NMOS, PMOS, and isolation structures, giving better fits not only to the absolute value of V_{th} and leakage current, but also to the V_{th} trends with respect to substrate bias and gate length.

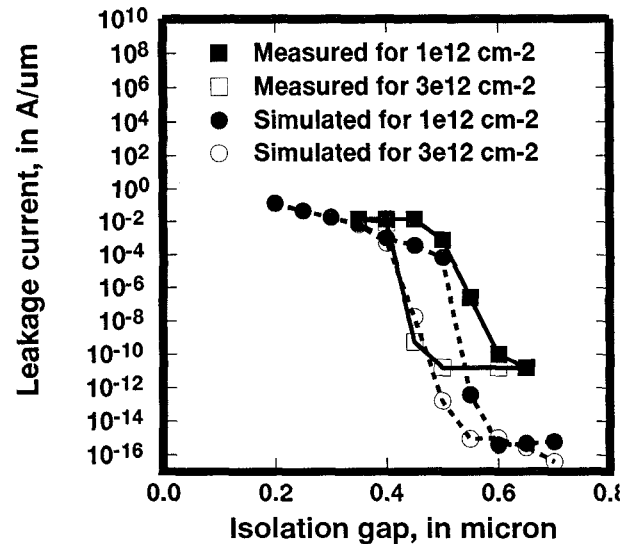


Figure 7: Leakage current across the isolation structure in Figure 5, as a function of the lithographic isolation gap. The symbols for the experimental data are open squares for phosphorus tub implant dose of 3e12 cm⁻², and filled squares for 1e12 cm⁻². Simulated data, using PROPHET with the P dose loss model and PADRE device simulator, are shown as circles. The agreement is reasonable, given the measurement lower limit of 1e-11 A/μm.

REFERENCES

- [1] P. B. Griffin, S. W. Crowder, and J. M. Knight, "Dose loss in phosphorus implants due to transient enhanced diffusion and interface segregation". *Appl. Phys. Lett.*, vol. 47, pp. 482-484 (1995).
- [2] F. Lau, L. Mader, C. Mazure, Ch. Werner, and M. Orlowski, "A model for phosphorus segregation at the silicon-silicon dioxide interface", *Appl. Phys. A.*, vol. 49, p.671 (1989).
- [3] Y. Sato, M. Watanabe, and K. Imai, "Characterization of Phosphorus Pile-up at the SiO₂/Si interface", *J. of Electrochem. Soc.*, vol. 140, pp. 2679-2682 (1993).
- [4] E. H. Nicollian and A. Chatterjee, *J. Electrochem. Soc.*, vol. 141, p. 2182 (1994).
- [5] M. R. Pinto, D. M. Boulin, C. S. Rafferty, R. K. Smith, W. M. Coughran, I. C. Kizilyalli, M. J. Thoma, "Three-dimensional characterization of mbipolar transistors in a submicron BiCMOS technology using integrated process and device simulation", *IEDM 1992*, pp. 923-926 (1992).
- [6] C. S. Rafferty, H-H Vuong, S. A. Eshraghi, M. D. Giles, M. R. Pinto, and S. J. Hillenius, "Anomalous short-channel threshold voltage due to transient enhanced diffusion", *IEDM 1993*, pp. 311-314 (1993).
- [7] H.-H. Vuong, C. S. Rafferty, S. A. Eshraghi, J. L. Lentz, P. M. Zeitoff, M. R. Pinto, and S. J. Hillenius, "Effects of oxide interface traps and Transient Enhanced Diffusion on the process modeling of PMOS devices", *IEEE Trans. Elec. Dev.*, vol. 43, pp. 1144-1152 (1996).
- [8] M. D. Giles, "Transient phosphorus diffusion below the amorphization threshold", *J. Electrochem. Soc.*, vol. 138, pp. 1160-1165 (1991).